

# TIME-FREQUENCY CARDIAC PASSIVE ACOUSTIC LOCALIZATION

Y. Bahadırlar<sup>1</sup>, H. Ö. Gülcür<sup>2</sup>

<sup>1</sup>TÜBİTAK Marmara Research Center, Information Technologies Research Institute, Kocaeli, Turkey

<sup>2</sup>Institute of Biomedical Engineering, Boğaziçi University, İstanbul, Turkey

**Abstract-** In a previous work, the authors have used a novel, radically different approach based on concurrent multi-sensor array measurements and “super-resolution” array processing scheme for phonocardiographic signals. Using a specially designed passive acoustic array, acoustic “images” corresponding to the various distinct phases of the heartbeat were obtained. In this paper, this approach is extended using a novel framework, called Time-Frequency Cardiac Passive Acoustic Localization (TF-CARDIOPAL). The Choi-Williams distribution is utilized to calculate a spatial time-frequency matrix to characterize the spatial time-frequency distribution for the nonstationary array signals. Distinctive components of this matrix on the time-frequency plane yield important clues on possible source locations in the heart. This finding has been used in extracting localization information from the first heart sound signals from a healthy human subject. Meaningful source localization results that are well correlated with the mechanical activation of the heart are obtained.

**Keywords** - Heart sounds, array processing, time-frequency distributions, cardiac acoustic imaging

## I. INTRODUCTION

In medicine, phonocardiography has been used as a noninvasive diagnostic tool in screening patients with cardiac problems. It has kept its popularity up to the early 1980's, but lost ground in favor of recently developed imaging techniques such as CT, MRI and ultrasound. Advanced spectral estimation and signal processing methods applied to sensitive phonocardiogram (PCG) data re-emphasized the importance of the technique. Significance of PCG and the signal processing methods for the diagnosis of the heart valve dysfunction and degeneration are strongly established in [1], [2]. However, conventional techniques using single channel PCG data do not have spatial information concerning the heart sounds. Locating the sounds in the thorax could improve the diagnosis of the heart abnormalities and help in solving the controversy on the exact origin of the heart sounds.

Recently, several researchers have directed their efforts to achieve a spatial mapping of the acoustic energy emitted by the heart. In these investigations, the heart sounds are acquired from certain conventional landmarks on the thorax. They are then processed using coherent averaging and interpolation of the acoustic energy among the cardiac sensors [3], [4]. In our previous work, we used a novel, radically different approach based on concurrent multi-sensor

array measurements and “super-resolution” array processing on the PCG signals [5]. Our approach stems from the modern perspective on the genesis of the heart sounds proposed by Durand and Guardo; namely the multi-degree of freedom theory [1].

In the previous work, a system called Cardiac Passive Acoustic Localizer (CARDIOPAL for short) was developed for spatial localization of the assumed acoustic sources of the heart. This system consisted of a specially designed passive acoustic array, instrumentation hardware and a 2-D array processing software. A subspace based adaptive array processing method called MUSIC algorithm along with a signal model for the sound-source foci on the heart and the propagation of the sounds to the chest was used. Effectiveness of the method was investigated using extensive recording at different SNR levels on phantoms and tested with success on adult subjects as well as on pregnant women [6]. Using this system, different “images” corresponding to the various distinct phases of the heart beat; e.g., closure of the mitral and tricuspid valves, ejection of the blood in systole, closure of the aortic and pulmonary valves, early and late diastole, were obtained.

In this work, we extend our previous method using novel framework, called Time-Frequency Cardiac Passive Acoustic Localization (TF-CARDIOPAL). In this framework, to characterize the spatial time-frequency distribution for the nonstationary array signals the Choi-Williams distribution (CWD) is utilized and a spatial time-frequency matrix is calculated. Besides having the same properties as the other distributions, this matrix has very good suppression of cross terms and a very good resolution [7]. Characteristic components of this matrix on the time-frequency plane yield important clues on likely source locations in the heart. This finding has been used in processing the first heart sound signals from a healthy human subject to extract localization information concerning the acoustic sources.

## II. METHODOLOGY

### A. 2-D Microphone Array and the Instrumentation System

The multi-sensor cardiac probe is a 105 mm x 105 mm x 40 mm planar microphone array consisting of 16 miniature electret microphones mounted on a 4 x 4 grid. A soft polyurethane layer is used to couple the rigid surface of the collimator of the array to the thorax. The data acquisition hardware of the system consists of microphone amplifiers, 80-1000 Hz band-pass analog filters, analog-digital-converters and hardware interface to a PC. During the analog-to-digital conversion process, all microphone channels are sampled simultaneously and quantized using 12 bits. Data is transferred to the PC via Direct Memory Access (DMA).

Report Documentation Page		
<b>Report Date</b> 25OCT2001	<b>Report Type</b> N/A	<b>Dates Covered (from... to)</b> -
<b>Title and Subtitle</b> Time-Frequency Cardiac Passive Acoustic Localization		<b>Contract Number</b>
		<b>Grant Number</b>
		<b>Program Element Number</b>
<b>Author(s)</b>		<b>Project Number</b>
		<b>Task Number</b>
		<b>Work Unit Number</b>
<b>Performing Organization Name(s) and Address(es)</b> TÜBÝTAK Marmara Research Center, Information Technologies Research Institute, Kocaeli, Turkey		<b>Performing Organization Report Number</b>
<b>Sponsoring/Monitoring Agency Name(s) and Address(es)</b> US Army Research, Development & Standardization Group (UK) PSC 802 Box 15 FPO AE 09499-1500		<b>Sponsor/Monitor's Acronym(s)</b>
		<b>Sponsor/Monitor's Report Number(s)</b>
<b>Distribution/Availability Statement</b> Approved for public release, distribution unlimited		
<b>Supplementary Notes</b> Papers from the 23rd Annual International Conference of the IEEE Engineering in Medicine and Biology Society, October 25-28, 2001, held in Istanbul, Turkey. See also ADM001351 for entire conference on cd-rom.		
<b>Abstract</b>		
<b>Subject Terms</b>		
<b>Report Classification</b> unclassified		<b>Classification of this page</b> unclassified
<b>Classification of Abstract</b> unclassified		<b>Limitation of Abstract</b> UU
<b>Number of Pages</b> 4		

### B. Acoustic Array Signal Model

Assuming that there are  $K$  point sources in the near field of the  $4 \times 4$ -element array, the model for the signal  $X_{mn}(t)$  at  $(m, n)$ 'th microphone is written as

$$X_{mn}(t) = \sum_{k=1}^K S_k(t) a_{mn}(t, \mathbf{r}_k) + n_{mn}(t),$$

$$1 \leq m \leq M, 1 \leq n \leq N; \quad (1)$$

where  $S_k(t)$  is the waveform of the  $k$ 'th sound source,  $a_{mn}(t, \mathbf{r}_k)$  is the time-varying steering parameter depending on the  $k$ 'th source, on the array geometry, and  $\mathbf{r}_k = (r_{ok}, \theta_k, \phi_k)$  is the spherical ordinate vector of the  $k$ 'th source with respect to the array origin.  $n_{mn}(t)$  is spatially white Gaussian noise,  $M$  and  $N$  are the number of microphones in the axis of the planar array.

Two fundamental assumptions can reasonably be made on the production and the propagation of the heart sounds as in the previous work [5], [6]. *Assumption 1*: The vibrating tissue is small compared to the size of the microphone array and acts as a point source, therefore, the sound wave from the heart tissue propagate as a spherical wave in the near field. *Assumption 2*: The intervening tissue is homogenous in terms of sound absorption characteristics. The steering parameter  $a_{mn}(t, \mathbf{r}_k)$  can be formed based on these assumptions and another parameter due to the delay/advance of the wave with respect to the array origin:

$$\begin{aligned} a_{mn}(t, \mathbf{r}_k) &= \left( \frac{r_{ok}}{d_{mn}(\mathbf{r}_k)} \right)^2 \\ &\cdot \exp(-(\rho d_{mn}(\mathbf{r}_k) / r_{ok} + j\kappa(r_{ok} - d_{mn}(\mathbf{r}_k)))), \\ d_{mn}(\mathbf{r}_k) &= \left( r_{ok}^2 + x_m^2 + y_n^2 - 2r_{ok} \sin \theta_k (x_m \cos \theta_k + y_n \sin \phi_k) \right)^{1/2} \\ x_m &= (m - (M+1)/2)d_x, y_n = (n - (N+1)/2)d_y, \\ \kappa &= 2\pi f(t)/(c/d_x), d_x = d_y, \end{aligned} \quad (2)$$

where  $r_{ok}$  is the distance between the  $k$ 'th source and the array origin,  $d_{mn}(\mathbf{r}_k)$  is the distance from the same source to the  $(m, n)$ 'th array element,  $\theta_k$  and  $\phi_k$  is the elevation and azimuth angles, respectively.  $\kappa$  is the wave number depending on time-varying frequency of the source ( $f(t)$ ) and on the speed of the sound ( $c$ ) on the medium,  $d_x$  and  $d_y$  are the inter-element distances in the respective axes on the array,  $\rho$  is the exponential loss factor of the medium.

### C. A Spatial Time-Frequency Distribution

In the previous work, it was shown that the phase-shift parameter contributes less to the localization than the other two parameters [5], [6]. Therefore neglecting the phase-shift parameter in (2), one can obtain the time-independent array steering parameter, i.e.,  $a_{mn}(\mathbf{r}_k)$ . Additionally, the time-independent steering parameter assumes that a source does not change its position through an estimation interval. In matrix form (1) can be written as the following:

$$\mathbf{X}(t) = \mathbf{AS}(t) + \mathbf{n}(t), \quad (3)$$

where  $\mathbf{X}(t)$  is the  $MN \times 1$  array output vector,  $\mathbf{A} = [\mathbf{a}(\mathbf{r}_1), \mathbf{a}(\mathbf{r}_2), \dots, \mathbf{a}(\mathbf{r}_K)]$  is the  $MN \times K$  steering matrix correspondingly defined by the steering parameters  $a_{mn}(\mathbf{r}_k)$ ,  $\mathbf{S}(t) = (S_1(t), S_2(t), \dots, S_K(t))^T$  is the  $K \times 1$  source magnitude vector and  $\mathbf{n}(t) = (n_1(t), n_2(t), \dots, n_K(t))^T$  is the  $MN \times 1$  spatial white noise vector.

The discrete form of the Choi-Williams Distribution (CWD) can be written as the following:

$$\begin{aligned} E_U(t, f) &= 2 \sum_{\tau=-\infty}^{\infty} W_T(\tau) e^{-2\pi f\tau/T} \\ &\cdot \left[ \sum_{\mu=-V/2}^{V/2} \frac{W_U(\mu)}{\sqrt{4\pi\tau^2/\sigma}} \exp\left(-\frac{\mu^2}{4\tau^2/\sigma}\right) \right. \\ &\left. \cdot U(n+\mu+\tau) U^*(n+\mu-\tau) \right], \end{aligned} \quad (4)$$

where  $U(\cdot)$  is the analytic signal used to prevent the aliasing effects [7].  $W_T(\tau)$  is a symmetrical window for the range of  $-T/2 \leq \tau \leq T/2$  and  $W_U(\mu)$  is a rectangular window with a value of 1 for the range of  $\mu$ . The size of the window  $W_T(\tau)$  determines a tradeoff between the frequency resolution of the signal auto-terms and the smoothed signal cross-terms. Denoting the kernel in the parenthesis of (4) by  $CW(\mu, \tau, \sigma)$ , inserting (3) into (4) and taking the expectation one obtains the discrete form of the spatial CWD:

$$\begin{aligned} \mathbf{D}_X(t, f) &= \mathbf{A} \mathbf{D}_S(t, f) \mathbf{A}^H + \sigma^2 \mathbf{I}, \\ \mathbf{D}_S(t, f) &= \\ &\left\{ 2 \sum_{\tau=-\infty}^{\infty} W_T(\tau) e^{-j2\pi f\tau/T} \right. \\ &\left. \cdot \sum_{\mu=-V/2}^{V/2} W_U(\mu) CW(\mu, \tau, \sigma) \mathbf{S}(t+\mu+\tau) \mathbf{S}^*(t+\mu-\tau) \right\}, \end{aligned} \quad (5)$$

where  $\mathbf{D}_S(t, f)$  is the source time-frequency matrix whose diagonal elements are the source auto-terms and the off-diagonal entries are the cross-time-frequency distribution of the source signals. CWD is a real-valued distribution, therefore  $\mathbf{D}_S(t, f)$  is a real-valued matrix. If  $\mathbf{D}_S(t, f)$  is also nonsingular and has rank  $K$ , the conventional MUSIC algorithm can directly be applied to equation (5), [5], [8]. However, the spatial distribution matrix  $\mathbf{D}_X(t, f)$  is not guaranteed to be a symmetric matrix. Therefore, the SVD has to be performed in the subspace analysis.

### D. Sample Spatial Time-Frequency Distribution

Ten segments of the first sound are extracted from the records of a healthy subject. The segments are then coherently averaged to get less noisy signal and the sample spatial distribution matrix  $\hat{\mathbf{D}}_X(t, f)$  is calculated using this signal. The four diagonal entries of the matrix corresponding to the sensors around the array origin are also averaged to get

a representative TFD of the isolated data. The sample spatial distribution matrix particular to a region is calculated using the following equation:

$$\hat{\mathbf{R}}_X = \frac{1}{TF} \sum_{t=t_1}^{t_T} \sum_{f=f_1}^{f_F} \hat{\mathbf{D}}_X(t, f), \quad (6)$$

where  $t_1$ ,  $t_T$  and  $f_1$ ,  $f_F$  define a region  $\Omega$  on the time-frequency plane.

### III. RESULTS

The average S1 signal from a sensor close to the array origin and the average TFD over the four channels around the array center are shown in Fig. 1 and Fig. 2, respectively. A cross-term free spatial TFD is obtained using 128 and 28 samples for the window length T and V, respectively and by assigning  $\sigma=1$ . Six regions of interests ( $\Omega$ s) are defined by inspecting the potential features of the TFD plane, as indicated in Fig. 2. As in our previous work, the number of sources and the loss factor in (1) and (2) are assigned to  $K = 5$  and  $\rho = 8$ , respectively and these values are kept constant in all calculations [5], [6]. Fig. 3 shows the localization results corresponding to each region and two additional estimates, which are due to a sum of early components. The source planes are defined on a  $50 \times 50$  grid (with  $2.5 \text{ mm} \times 2.5 \text{ mm}$  grid size) at 5-6 cm distal to the array plane. The estimates in Fig. 3 provide important spatial details that can be associated to mechanical activity of the heart during S1.

### IV. DISCUSSION

A principal focus in the middle of estimates is consistently observed in early stages of S1, i.e., in region  $\Omega_1$ ,  $\Omega_2$  and  $\Omega_3$ . In general, this may be related to the phenomena emphasized by cardiohemic theory [1], [2]. The region  $\Omega_3$  shows also a good clue for the closure of the mitral valve beneath the principal focus. This focus seems to shifts slightly to the left side in region  $\Omega_4$ , towards the tricuspid area. The region  $\Omega_5$  exerts a good focus of the closure of the tricuspid valve. The weak components in region  $\Omega_6$  result in two foci that may be associated to the opening snaps of the pulmonary and aortic valves. There is still a very weak activity at the tricuspid area.

Similar results from another subject with mild valvular dysfunction were also obtained. In this way, the second heart sound signals (S2) from both subjects were also investigated and meaningful results were achieved. However, these results could not be given here due to the space limitations.

### V. CONCLUSION

In this paper, a novel approach, called Time-Frequency Cardiac Passive Acoustic Localization (TF-CARDIOPAL) is discussed for obtaining acoustic “images” that show 2-D distribution of assumed “point” source locations within the body. The approach is based on using multi-sensor array measurements of heart sounds. To characterize the spatial time-frequency distribution of the nonstationary array signals, the Choi-Williams distribution is utilized and a spatial time-frequency matrix is calculated. Distinctive components of this matrix on the time-frequency plane contain important clues on possible acoustic source locations in the heart. This finding has been used in extracting localization information from the multi-sensor array measurements of the first heart sound signals from a healthy human subject. Source localization results have been found to be well correlated with the mechanical activation of the heart. Although the method needs extensive and comparative studies to be useful for clinical applications, it has a good potential for clinical analysis and may shed new light on controversial issues concerning the genesis of the heart sounds.

### REFERENCES

- [1] L.-G. Durand and P. Pibarot, “Digital signal processing of the phonocardiogram: review of the most recent advancements,” *Critical Review in Biomedical Eng.*, vol. 23, pp 163-219, 1995.
- [2] R.M. Rangayyan and R.J. Lehner, “Phonocardiogram signal analysis: a review,” *CRC Critical Review in Biomedical Eng.*, vol. 15, pp 211-236, 1988.
- [3] J.C. Wood and D.T. Barry, “Quantification of first heart sound frequency dynamics across the human chest wall,” *Med. & Biol. Eng. & Comput.*, vol. 32, pp S71-S78, 1994.
- [4] M. Cozic, L.-G. Durand and R. Guardo, “Development of a cardiac acoustic mapping system,” *Med. & Biol. Eng. & Comput.*, vol. 36, pp 431-437, 1998.
- [5] Y. Bahadırılar and H.Ö. Gülcür, “Cardiac passive acoustic localization: CARDIOPAL,” *Turkish J. of Electrical Eng. & Comput.*, vol. 6, pp 243-259, 1998.
- [6] Y. Bahadırılar, *CARDIOPAL: Cardiac Passive Acoustic Localization and Mapping using 2-D Recordings of Heart Sounds*, Bogaziçi Univ. Institute of Biomedical Eng., PhD Thesis, June 1997.
- [7] H.-I. Choi and W.J. Williams, “Improved time-frequency representation of multicomponent signal using exponential kernels,” *IEEE trans. on Acoust., Speech, Signal, Processing*, vol. 37, pp 862-871, June 1989.
- [8] A.B. Gershman and M.G. Amin, “Wideband direction-of-arrival estimation of multiple chirp signal using spatial time-frequency distributions,” *IEEE Signal Processing Lett.*, vol. 7, pp 152-155, June 2000.

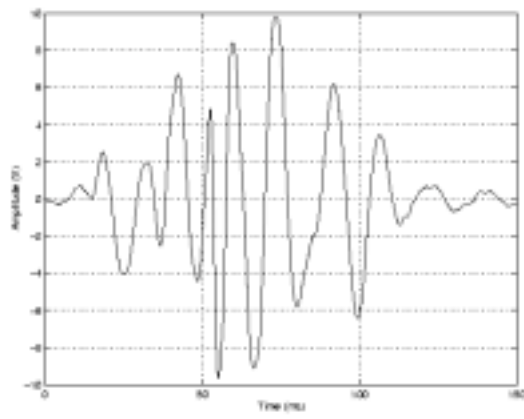


Fig.1. The average first heart sound signal from a healthy subject.

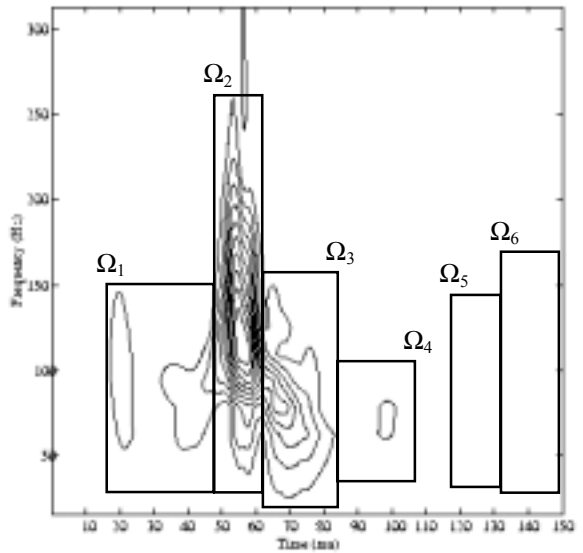


Fig.2. The average time-frequency distribution of the four channels (pre-filtered using 100 Hz high-pass FIR filter).

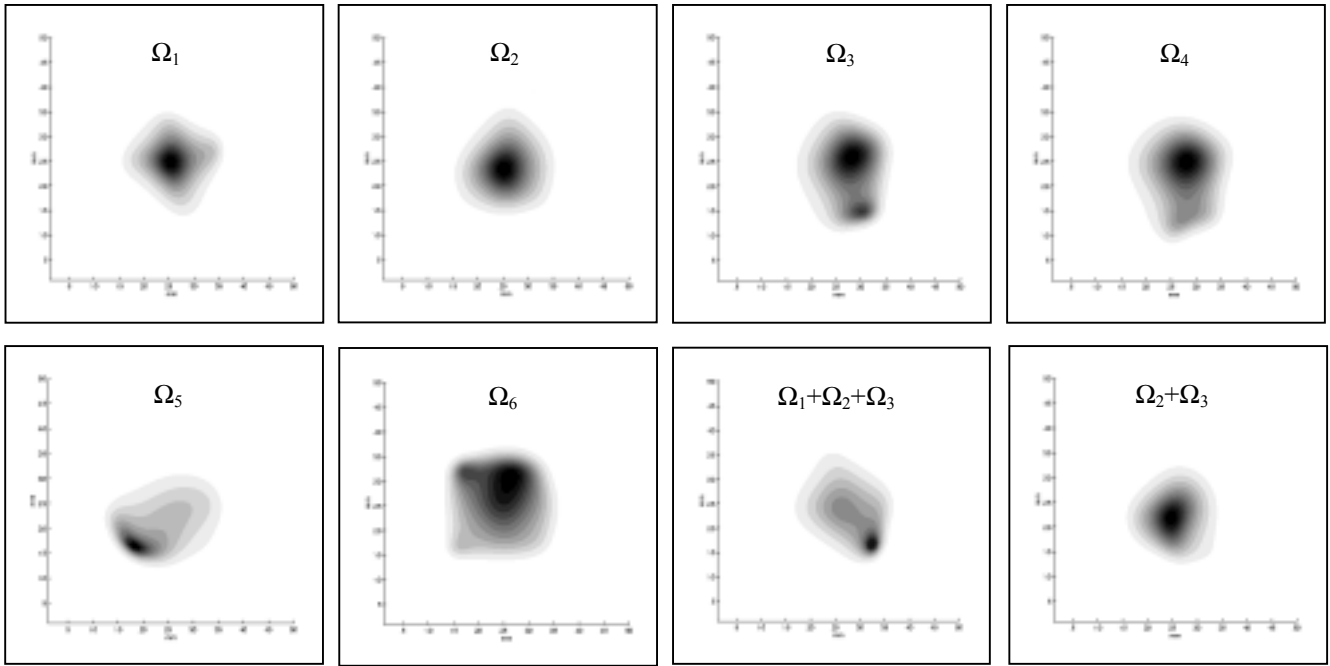


Fig. 3. Each source localization estimate relates a particular region defined on the time-frequency plane of the first heart sound.